

Three-dimensional Resistive MHD
Investigation of Spheromak Sustainment

Carl R. Sovinec, John M. Finn,
and Diego del Castillo-Negrete,

Los Alamos National Laboratory

presented at the

American Physical Society Centennial Meeting/
1999 International Sherwood Fusion Theory Conference

March 23, 1999

ACKNOWLEDGMENTS

NIMROD code development team and advisors:

Ahmet Aydemir	IFS
Curtis Bolton	OFES
James Callen	U-WI
Ming Chu	GA
John Finn	LANL
Tom Gianakon	LANL
Alan Glasser	LANL
Scott Kruger	SAIC
Jean-Noel Leboeuf	UCLA
Richard Nebel	LANL
Steve Plimpton	SNL
Nina Popova	MSU
Dalton Schnack	SAIC
Carl Sovinec	LANL
Alfonso Tarditi	SAIC

Computations have been performed at

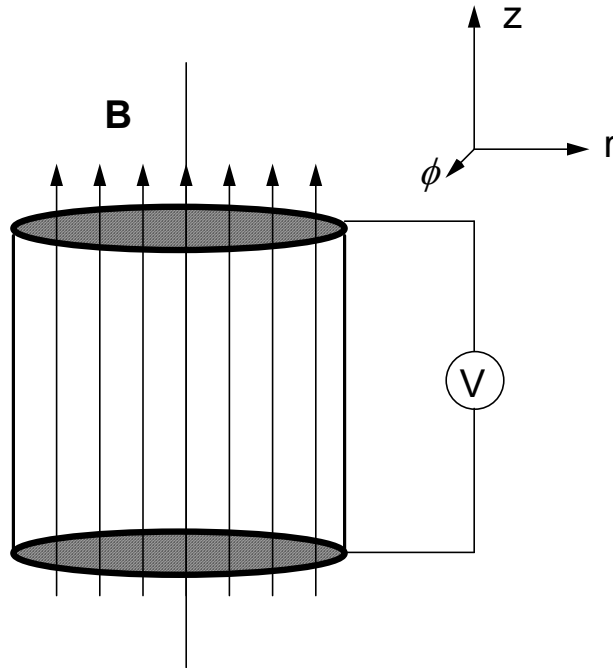
National Energy Research Scientific Computing Center, LBNL
Advanced Computing Laboratory, LANL

PREVIEW

- First (?) three-dimensional MHD simulations of spheromak sustainment are presented.
 - Earlier work by Katayama and Katsurai [Phys. Fluids **29**, 1939 (1986)], Sgro, Mirin, and Marklin [Phys. Fluids **30**, 3219 (1987)], and Horiuchi, Sato, and Uchida [Phys. Fluids B **4**, 672 (1992)] investigated nonlinear behavior during decay from a symmetric spheromak.
- Nonlinear activity converts toroidal flux to poloidal flux.
- Magnetic fields often exhibit chaotic scattering, but closed flux surfaces are demonstrated for:
 - weakly driven stellarator-like cases
 - decaying spheromak
- Limit cycle behavior exists in large current cases and larger S cases.

GEOMETRY AND EQUATIONS

The geometry for simulating a "flux core" or "electrode" spheromak is a simple can with magnetic flux frozen into the top and bottom ends, which represent electrodes.



The physical behavior of the system is modeled with the resistive MHD equations, where uniform density and vanishing pressure are assumed:

$$\rho \left(\frac{\partial \mathbf{V}}{\partial t} + \mathbf{V} \cdot \nabla \mathbf{V} \right) = \mathbf{J} \times \mathbf{B} + \nabla \cdot \rho \nu \nabla \mathbf{V}$$

$$\frac{\partial \mathbf{B}}{\partial t} = \nabla \times (\mathbf{V} \times \mathbf{B} - \eta \mathbf{J})$$

The equations are solved with the NIMROD simulation code.

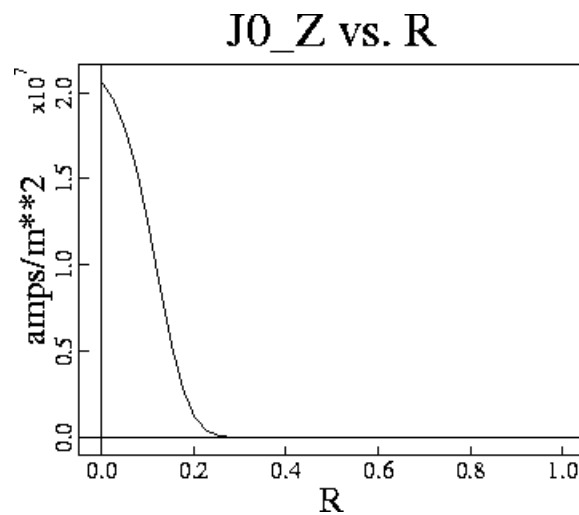
- Two-fluid or single-fluid MHD equations
- Finite elements in the poloidal plane
- Pseudospectral, Fourier series representation of the toroidal direction
- Semi-implicit time advance
- Message-passing communication among processors
- Now publicly available from
 - **<http://t15web.lanl.gov>**
 - Note: the web site has been recently changed due to LANL computer security upgrades!!

Simulation parameters:

- 1) Cylinder radius is 1 m.
- 2) Computations have been performed with cylinder height=0.75-1.5 m.
- 3) Most cases have $S=2000$ on-axis; some have $S=10,000$.
- 4) Most cases have $\nu = \eta/\mu_0 = 1 \text{ m/s}^2$.
- 5) Computations use *either* a "stabilized" pinch equilibrium *or* a simulated applied axial electric field.

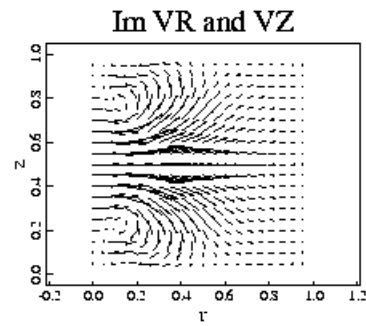
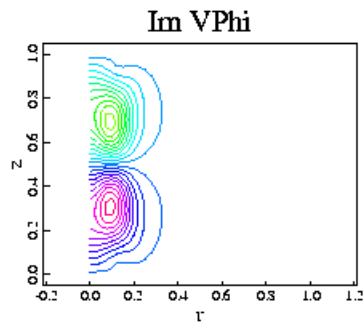
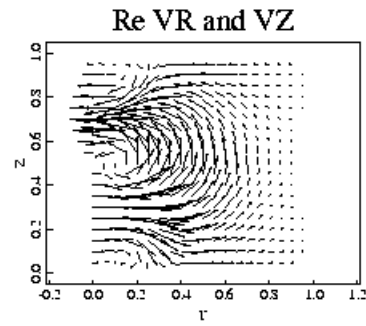
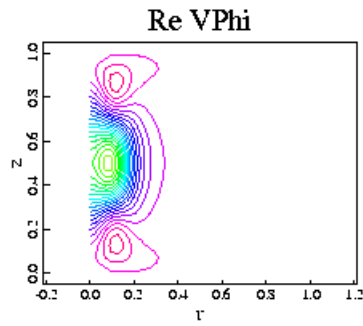
MHD INSTABILITY AND NONLINEAR SATURATION

- Enough current is drawn through the plasma such that a toroidally symmetric state is not maintained.
- Initial conditions represent an unstable "stabilized" z-pinch, where $\lambda \equiv \mu_0 \mathbf{J} \cdot \mathbf{B} / \mathbf{B}^2$ is larger than λ for a similarly sized RFP.



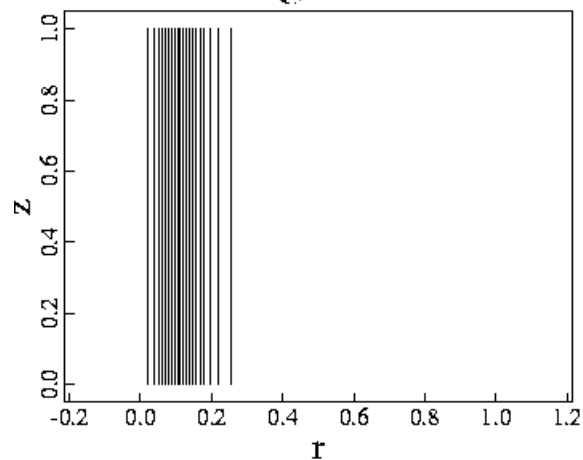
- The growth rate and eigenfunction of the linear (n=1) mode are strongly influenced by the field line tying conditions at the electrodes.

Auxiliary slide: plots of the $n=1$ linear eigenfunction.

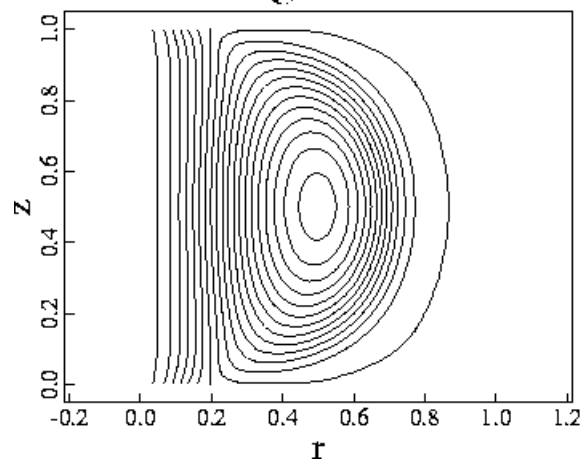


Saturation of the instability results from feedback to the $n=0$ field and from coupling to larger n .

Initial Average Poloidal Flux



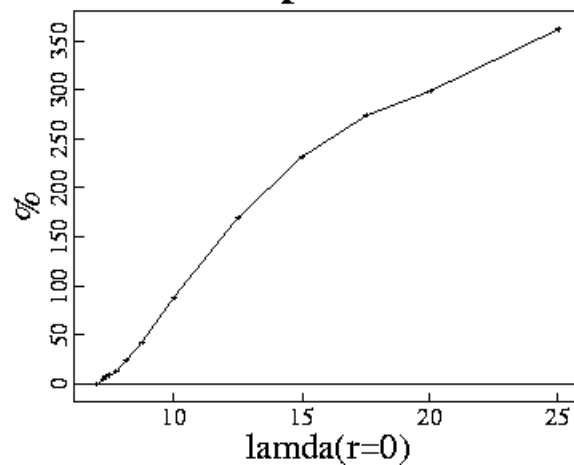
Final Average Poloidal Flux



- This case shows 170% amplification of the open poloidal flux. Results from a series of computations demonstrate increasing amplification with electrode current.

The following shows the nonlinear result of flux amplification vs. the on-axis parallel current (λ) of the equilibrium pinch for $S=2000$, $h=1$ m cases.

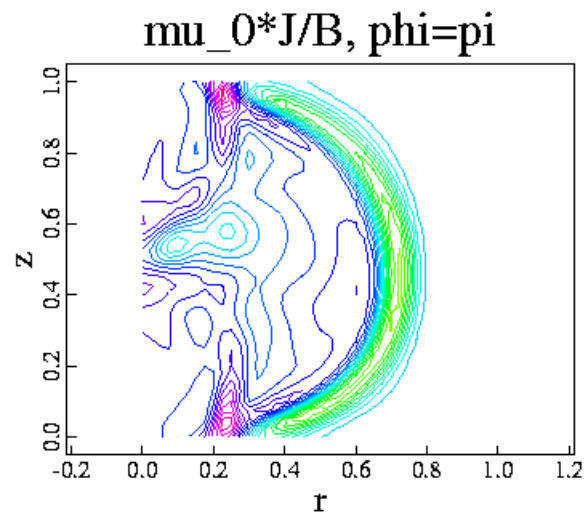
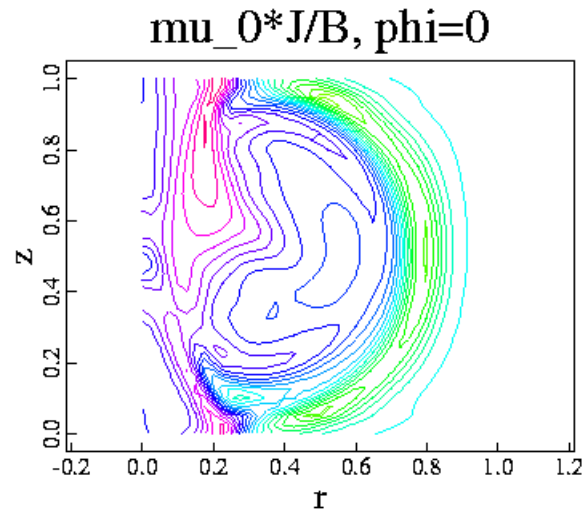
Poloidal Flux Amplification vs. Lambda



Auxiliary slide

The final saturated state is **NOT** a Taylor state.

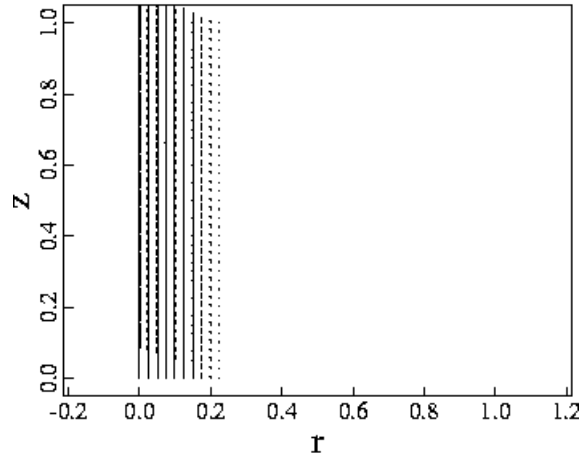
- While the parallel current (λ) on axis is reduced, $O(1)$ variations persist throughout.
 - The energy of the final state is greater than in the initial pinch.
 - The tightly wrapped magnetic field of the initial pinch restricts axial current.
 - The spatial fluctuations of the final state reduce the current density on axis, which partly unwraps the magnetic field, allowing more net axial current.
- ❖ This dissipative system is sustained, and it is not closed.
- ❖ Reorganization of the driven pinch results primarily from large-scale MHD activity, not from ubiquitous micro-tearing.



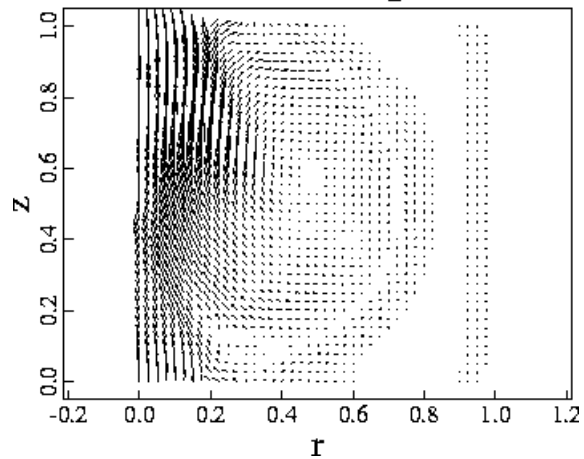
For the $\phi=0$ plot, the minimum value (green) is -8.8 and the maximum (red) is 13.7. For the $\phi=\pi$ plot, the minimum value is -12.4 and the maximum is 16.5.

Auxiliary slide

Pinch $J0_R$ and $J0_Z$



JR and JZ at $\phi=0$

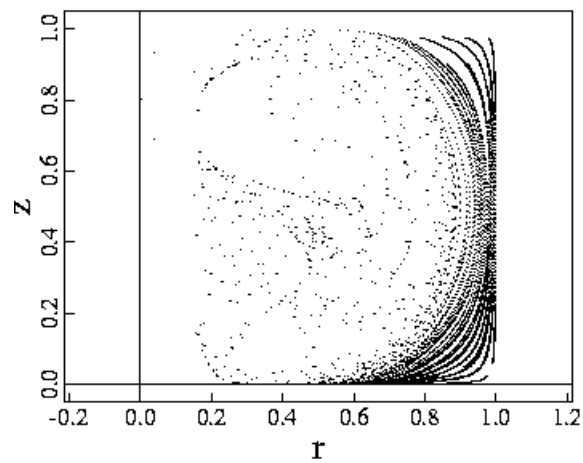


The maximum current density in the plot of the pinch is 31% larger than the largest vector in the $\phi=0$ plot, but the nonlinear state sustains 23% more current.

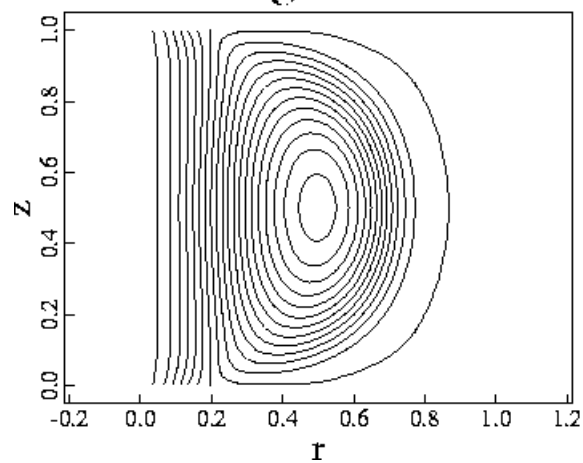
CHOATIC SCATTERING AND FLUX SURFACES

The robust generation of poloidal flux is usually accompanied by chaotic scattering of the magnetic field.

Poincare Surface of Section

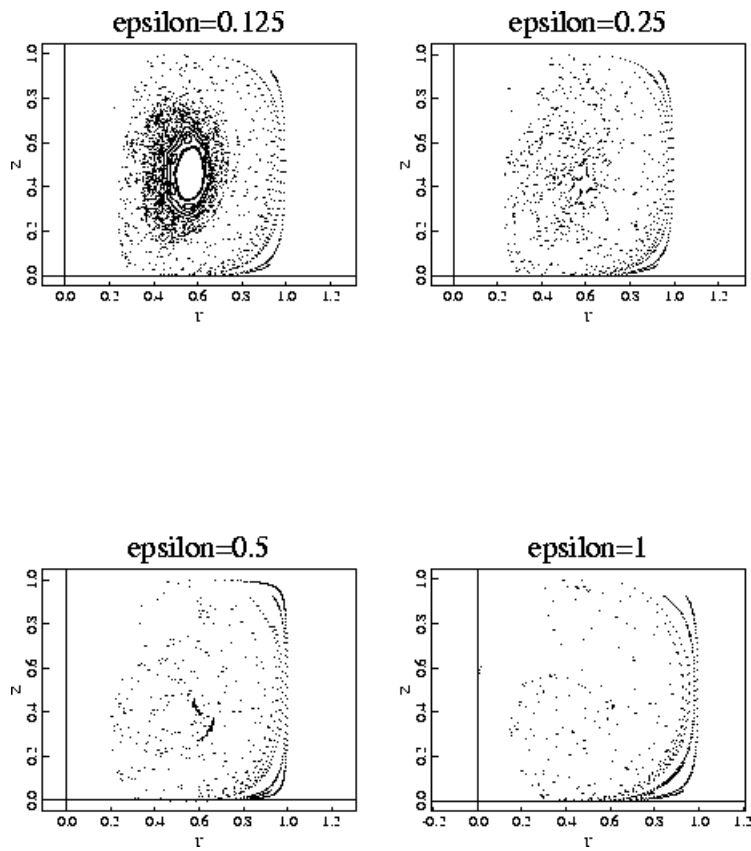


Final Average Poloidal Flux



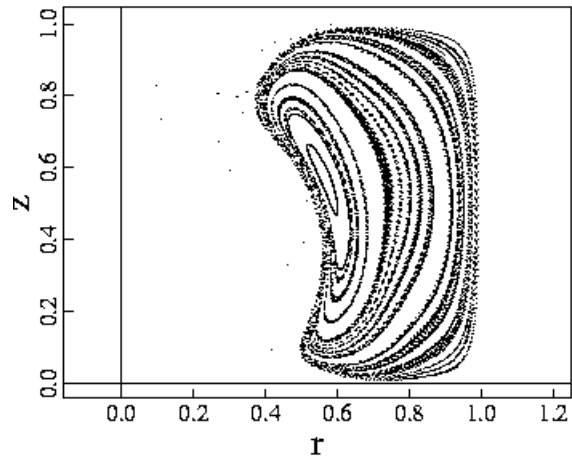
Auxiliary slide

Here we take the steady-state results from a case with $\lambda_{\text{pinch}}(0)=10$, multiply the nonsymmetric part of the magnetic field by factors < 1 , and redraw the surfaces of section.

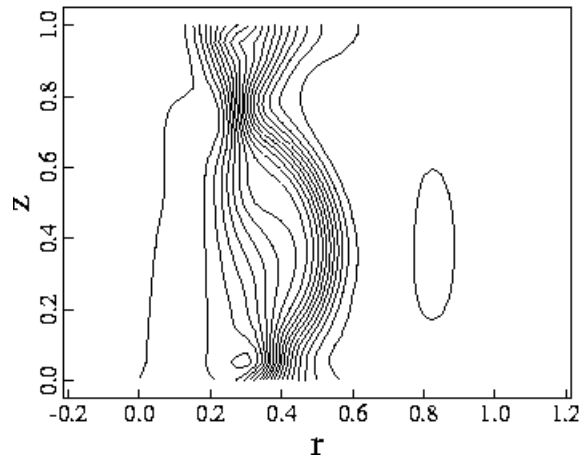


In weakly-driven cases, just above marginal stability, flux surfaces form and are sustained in steady state.

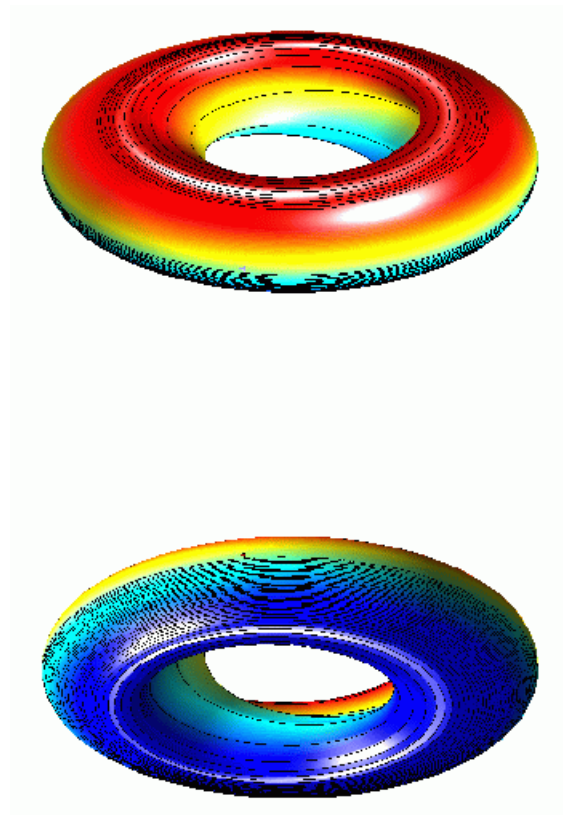
Poincare Surface of Section



$\mu_0 J/B$

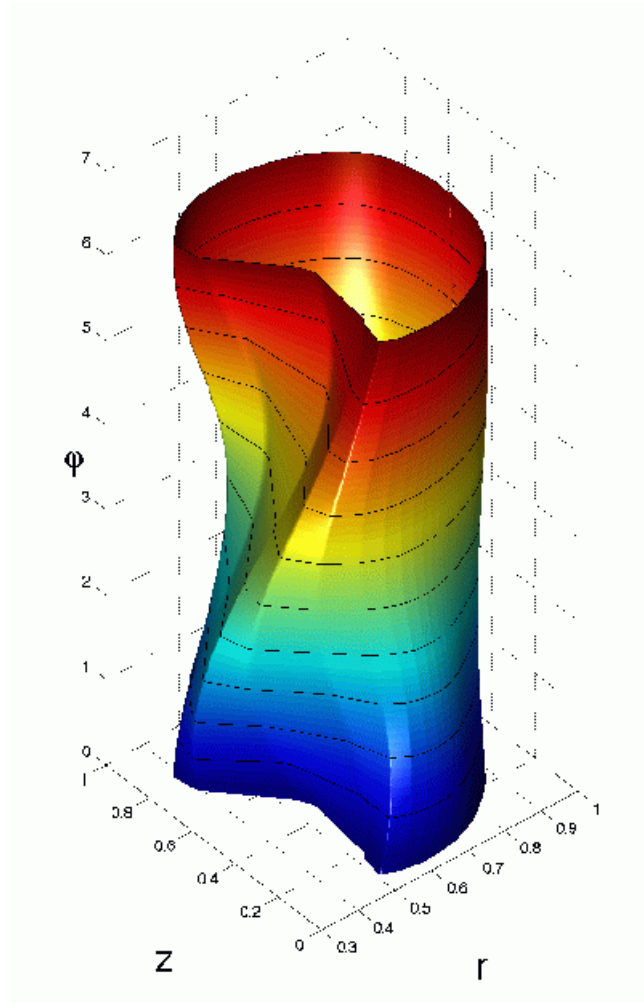


A field line trace over a flux surface shows that most of the transform occurs on the inner part of the surface.



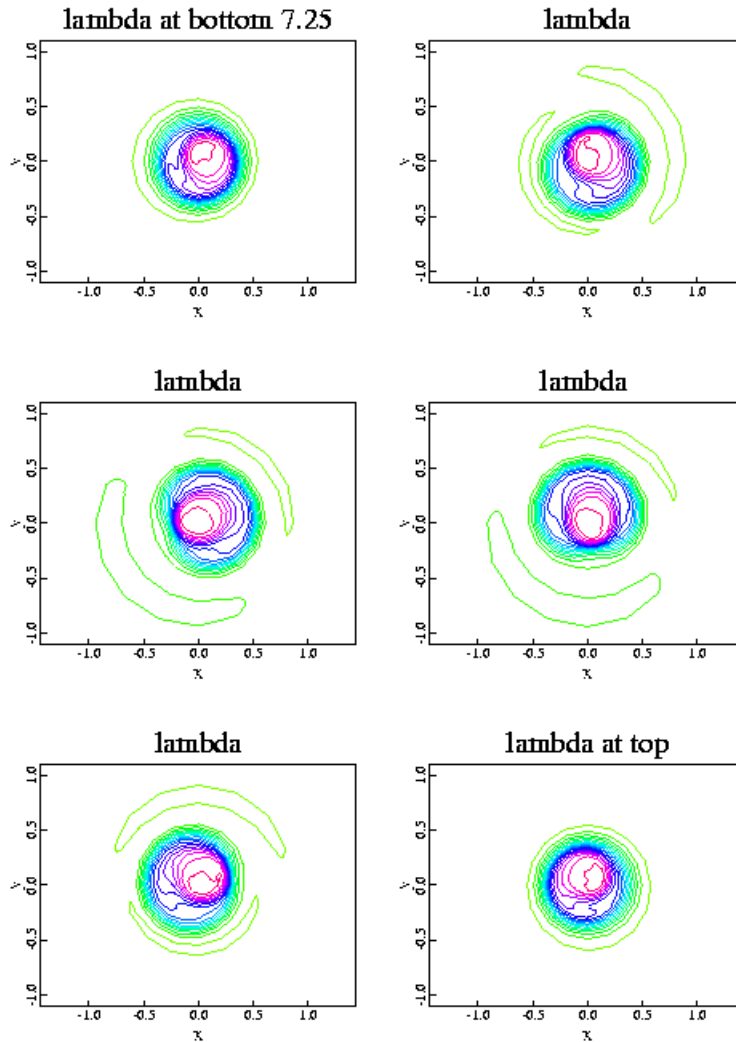
Color indicates axial position, z , on the surface.

A helical prominence exists on the inner part of the flux surface.
It coincides with helical pinch current at smaller r .



Color indicates toroidal position, ϕ , on the surface.

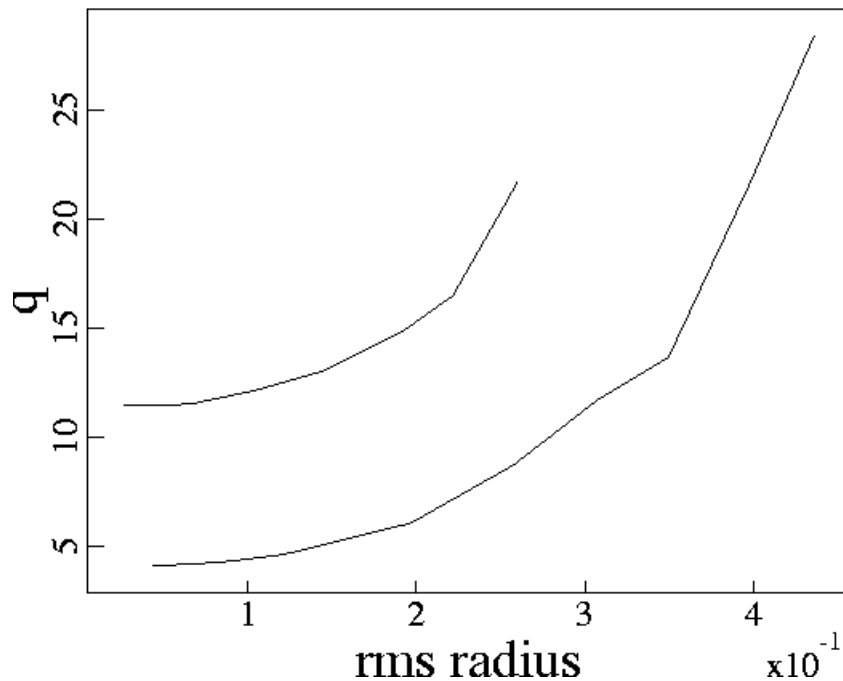
Auxiliary slide



Contours of λ at axial positions spaced from the bottom to the top of the can show the helically deformed pinch current.

Auxiliary slide

q vs. rms radius



The safety factor of the flux surfaces in a similar case is ~ 10 near the magnetic axis of the structure. q computed with just the symmetric ($n=0$) part of the field is in error by more than a factor of 2.

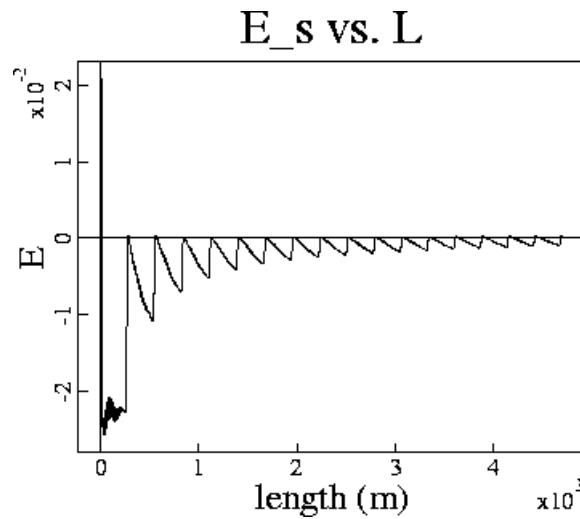
Note that the independent variable is $\langle r^2 \rangle^{1/2}$, mean square distance from the magnetic axis.

In steady state, flux surface averages of the electrostatic field vanish. This is satisfied in the computations.

$$\mathbf{B} \cdot \mathbf{E} = -\mathbf{B} \cdot \nabla \phi = \eta \mathbf{J} \cdot \mathbf{B}$$

$$\phi(L) - \phi(0) = -\int_0^L dl \frac{\eta \mathbf{J} \cdot \mathbf{B}}{B}$$

$$\lim_{L \rightarrow \infty} E_s(L) = 0, \quad E_s(L) \equiv \frac{\int_0^L dl \frac{\eta \mathbf{J} \cdot \mathbf{B}}{B}}{\int_0^L dl \frac{1}{B}}$$



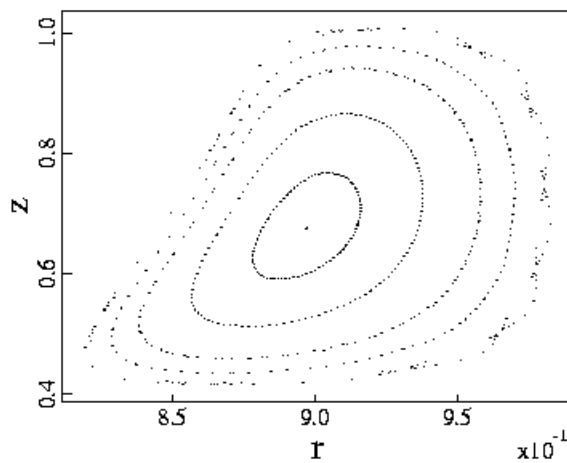
Due to the low current, we would not expect much Ohmic heating within these stellarator-like flux surfaces.

Auxiliary slide

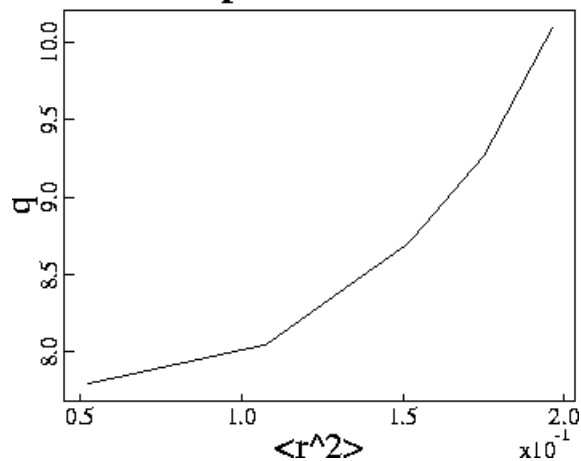
We are attempting to optimize the volume of flux surfaces and reduce q . One idea is to use a nonsymmetric perturbation of the magnetic field.

without nonsymmetric perturbation

Surface of Section



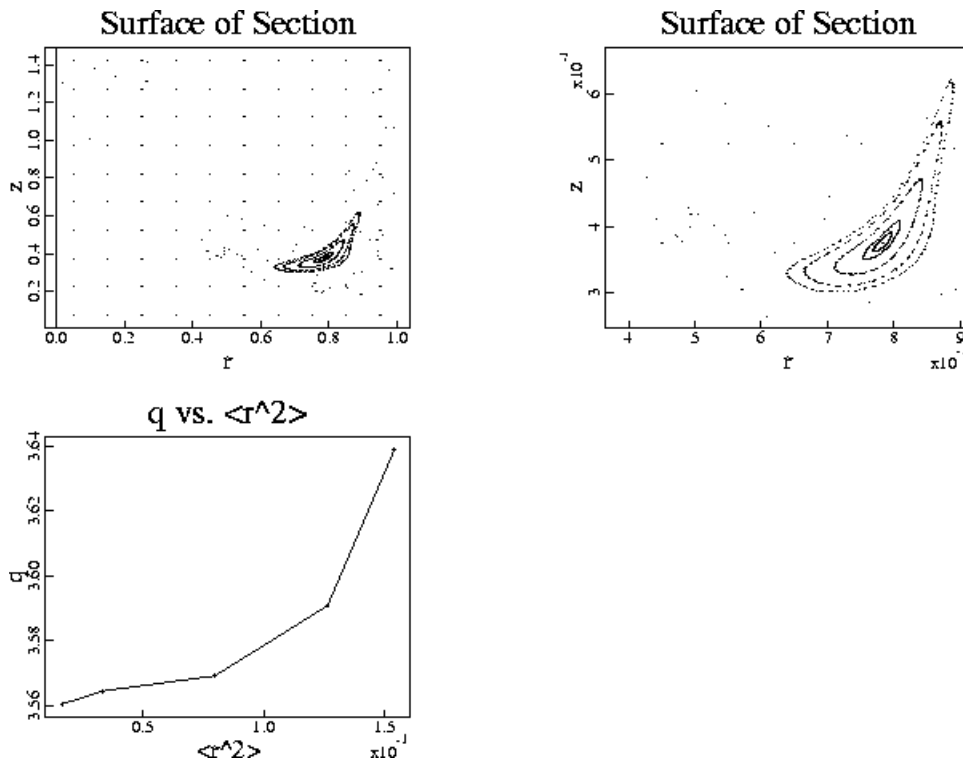
q vs. $\langle r^2 \rangle$



Note that the independent variable is $\langle r^2 \rangle^{1/2}$, mean square distance from the magnetic axis, not $\langle r^2 \rangle$.

Auxiliary slide

with nonsymmetric perturbation



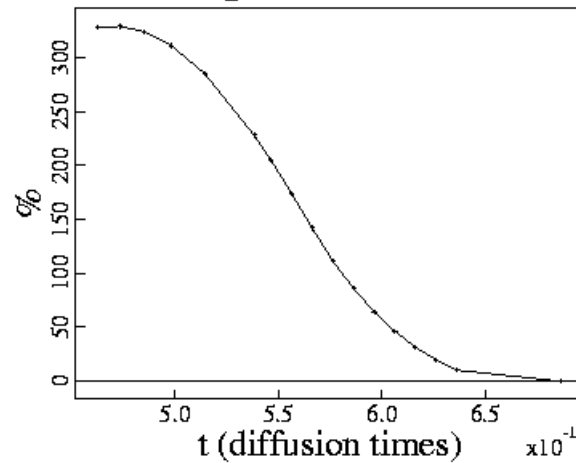
So far, we have been able to reduce q with the perturbation, but we have not yet increased the volume of flux surfaces.

Note that the independent variable is $\langle r^2 \rangle^{1/2}$, mean square distance from the magnetic axis, not $\langle r^2 \rangle$.

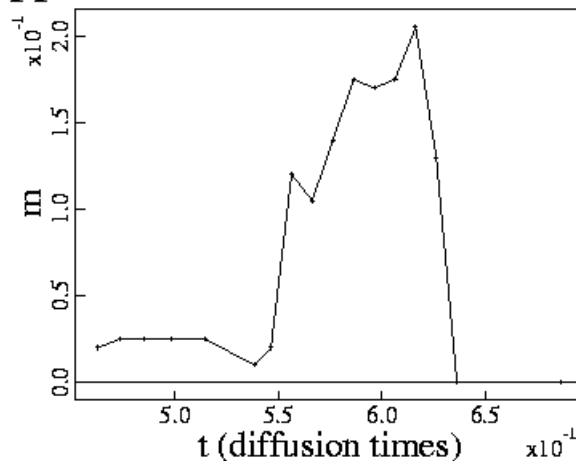
Flux surfaces have also been observed during decay.

When the applied potential is decreased over $0.1 \tau_r$ in a simulation with $h=1.5$ m and uniform flux through the electrodes, flux surfaces form as the poloidal field decays.

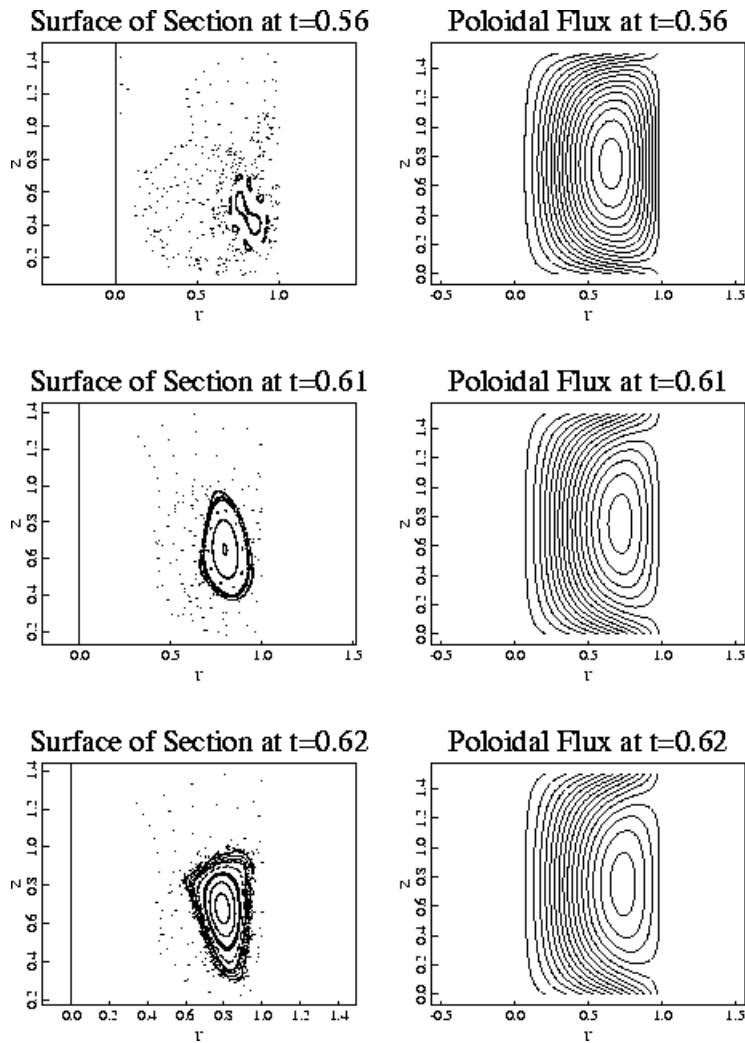
Flux Amplification vs. Time



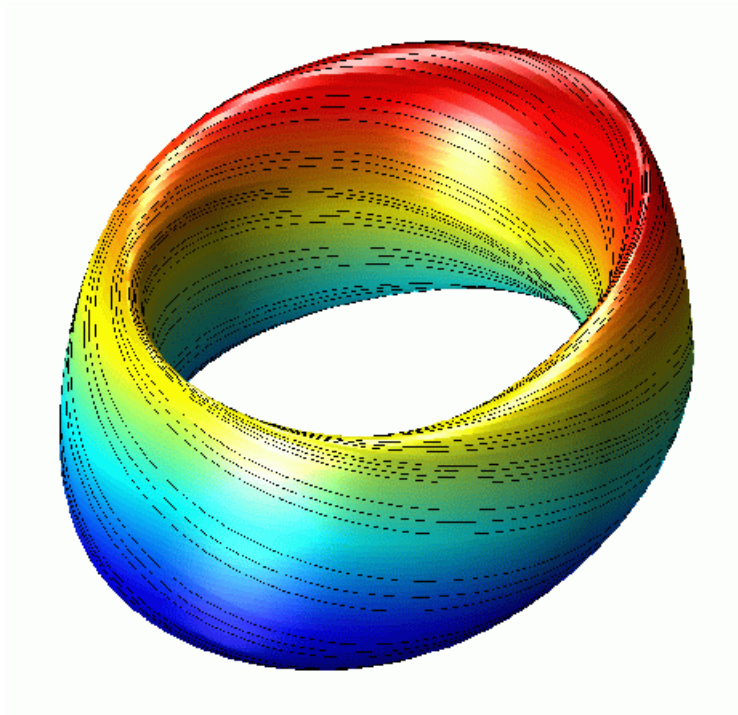
Appr. Island Minor Radius vs. Time



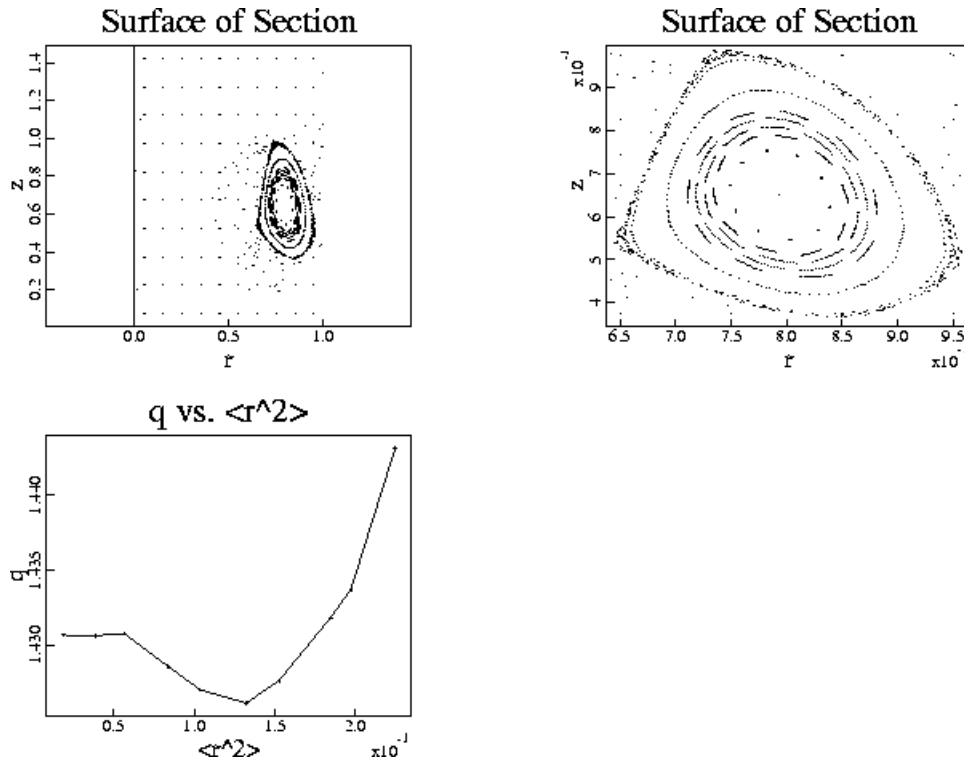
There is net toroidal electric field during the decay, which produces relatively uniform magnetic transform over the flux surfaces. It would also lead to Ohmic heating.



The transform on the flux surfaces formed by decay is much more uniform than in the weakly driven cases, and $q \sim 1$.



Auxiliary slide



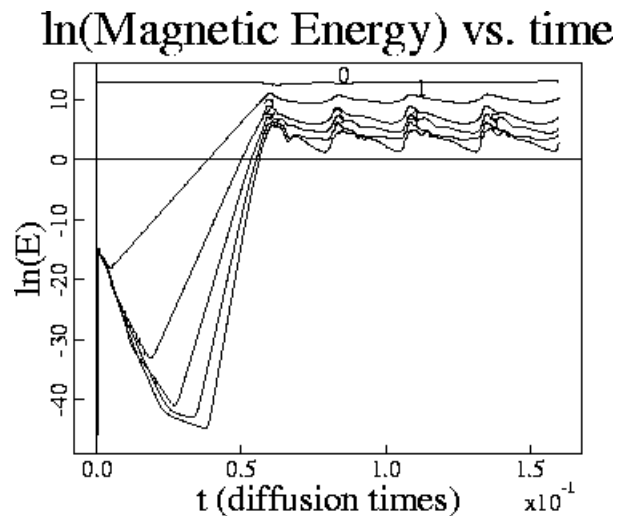
This plot shows the safety factor of a structure resulting from decay.

Note that the independent variable is $\langle r^2 \rangle^{1/2}$, mean square distance from the magnetic axis.

LIMIT CYCLE BEHAVIOR

In cases with larger S (10,000) or large current, a limit cycle is observed in the temporal evolution as the configuration is sustained.

The evolution of the magnetic energies of the different Fourier components in an $S=10,000$ demonstrates this behavior.



Small islands form at the low perturbed- \mathbf{B} point of the cycle.

CONCLUSIONS

- Results from 3D resistive MHD computations unambiguously show spheromak generation and sustainment. Large scale MHD activity converts toroidal flux to poloidal flux, "flux amplification."
- The sustained state is not a Taylor minimum energy state.
- Flux surfaces are observed to form:
 - Low current cases exhibit stellarator-like transform from current in the kinked pinch.
 - Decaying spheromaks show flux surfaces with net current. The plasma within these surfaces would have relatively good confinement, and it would be Ohmically heated. This may have bearing on the 400 eV temperatures observed during the decay phase of the CTX spheromak [Jarboe, et al., Phys. Fluids B **2**, 1342 (1990)].
- The limit cycle behavior observed in the larger S and large-current cases warrants further investigation.

FUTURE DIRECTIONS

- 1) More analysis of:
 - a) flux conversion process
 - b) limit cycle behavior
 - c) S dependence

- 2) Optimize the stellarator transform effect (nonsymmetric perturbations).

- 3) Investigate gun-driven configurations.

- 4) Investigate realistic geometries (SAIC-LLNL).